Positive–Negative Stiffness Actuators

David J. Braun, *Member, IEEE*, Vincent Chalvet, and Abhinav Dahiya

***Abstract*—Compliant actuators are typically designed to possess a tunable positive stiffness characteristic in order to generate restoring force upon displacement. These actuators either require two independent motor units or closed-loop control to change both their equilibrium position and output stiffness. The introduction of *negative stiffness*, in combination with tunable positive stiffness, may reduce the complexity and extend the capability of these actuators in unexpected ways. In this paper, we present a compliant actuator that employs a passive negative stiffness mechanism in conjunction with an effectively tunable positive stiffness mechanism. We show that such actuator enables open-loop stiffness modulation and equilibrium position control using a single motor unit, as opposed to more conventional variable stiffness and series elastic actuators. The paper presents the theoretical foundation of positive-negative stiffness actuators and demonstrates low-power stiffness modulation and equilibrium position control achievable with a prototype positive-negative stiffness actuator.**

***Index Terms*—Compliant actuators, negative stiffness mechanisms.**

I. Introduction

COMPLIANT actuators are commonly used to perform *equilibrium position* control for interaction-free manipulation, and *stiffness modulation* for safe human–robot [1], and stable robot–environment interaction [2]. In particular, series elastic actuators (SEAs) [3] use a single motor unit with feedback to simultaneously control the stiffness and the equilibrium position, while variable stiffness actuators (VSAs) [4], [5] use two separate motor units without feedback to achieve the same control capability. These actuators have been used in diverse applications, including human assistance and augmentation [6] and to drive complex biologically inspired robots [7].

Manuscript received July 11, 2018; accepted August 22, 2018. This paper was recommended for publication by Associate Editor J. Paik and Editor T. Murphey upon evaluation of the reviewers' comments. This work was supported by the SUTD-MIT International Design Center at the Singapore University of Technology and Design as part of the Energy-Efficient Compliant Actuator Designs project under Grant IDG31400108. This paper was presented in part at the IEEE International Conference on Robotics and Automation, Singapore, May 2017. *(Corresponding author: David J. Braun.)*

D. J. Braun is with the Dynamics and Control Laboratory, Singapore University of Technology and Design, Singapore 487372 (e-mail: david_braun@sutd.edu.sg).

V. Chalvet was with the Dynamics and Control Laboratory, Singapore University of Technology and Design, Singapore 487372. He is now with the National Engineering School of Saint-Étienne, Saint-Étienne 42100, France (e-mail: vincent.chalvet@enise.fr).

A. Dahiya was with the Dynamics and Control Laboratory, Singapore University of Technology and Design, Singapore 487372. He is now with the Department of Electrical and Computer Engineering, the University of Waterloo, Waterloo, ON N2L 3G1, Canada (e-mail: a4dahiya@uwaterloo.ca).

Color versions of one or more of the figures in this paper are available online at http://ieeexplore.ieee.org.

Digital Object Identifier 10.1109/TRO.2018.2872284

One of the main features of series elastic and variable stiffness actuators is the tunable *positive stiffness* that leads to a *unique* stable equilibrium position. Owing to this property, the actuator behaves similar to a helical spring [8], or a biological joint [9], as it tends to return back to its equilibrium position upon displacement. While this seems to be a desirable property, it limits the design space of most typical compliant actuators because positive stiffness actuators require two motor units or output position feedback to provide simultaneous equilibrium position control and stiffness modulation. It is known that output feedback can severely limit the achievable stiffness of SEAs [10], and also that the use of two motor units complicates the design of VSAs. Therefore, it may be promising to look for a new type of compliant actuator, one that may alleviate the above mentioned limitations, while still providing adequate control over the equilibrium position and the stiffness, which are both useful for robot control applications.

In this paper, we propose a new type of tunable positive–negative stiffness actuator (PNSA). This actuator combines a tunable positive-stiffness mechanism acting in parallel with a passive negative stiffness mechanism. The negative stiffness mechanism moves the actuator away from its equilibrium configuration, while the positive stiffness mechanism moves it back toward the equilibrium configuration. Depending on the two constituent mechanisms, the actuator can possess a large range of stiffness values, starting from finite negative stiffness and theoretically reaching up to positive infinity. Such a wide-range tunable PNSA has the following two distinct modes of operation: 1) stiffness modulation at its natural equilibrium configuration, and 2) equilibrium position control away from its natural equilibrium configuration. These two operation modes can be achieved using a single motor and without feedback of the output position. The same is not possible on more conventional SEAs and VSAs, even if one aims to separately modulate the equilibrium position and stiffness during the motion.

Passively or actively tunable negative stiffness mechanisms have been used in several previous designs [11]–[14]. The elastic element and key component in these designs is a buckling beam. By applying a large enough compressive force, negative stiffness is generated in the lateral direction of the beam. This leads to an instability phenomenon known as Euler's buckling [15]. In order to generate the compressive force, these designs use electric motors or piezoelectric actuators as force generators in the load path. Maintaining or changing the negative stiffness in this way requires large force and nonzero power. The actuator we propose has a fundamentally different means to maintain and change the negative stiffness. Namely, instead of actively generating the negative stiffness by a large control force, we employ

a passive negative stiffness mechanism, which does not require any control force [16], [17]. This allows us to displace the motor from the load path, and to replace a tunable negative stiffness mechanism that requires large motor force with a tunable positive stiffness mechanism, which requires a comparatively low motor force [18]–[20]. As a result, the actuator can significantly reduce the power required to change the negative stiffness, even when it is externally loaded and displaced from its equilibrium position.

The proposed actuator is similar to some of the recently developed clutch-based actuators [22], [23] in that, it can modulate both the stiffness and the equilibrium position using a single motor. However, unlike designs that employ a controllable clutch to switch between these two modes of operation, the proposed actuator relies on nonlinearity induced bifurcation. In particular, the motor unit can be used to switch between equilibrium position control and stiffness modulation as the stiffness of the actuator passes through zero during the motion. This bifurcation-based switching is used to eliminate a controllable clutch from the proposed actuator.

In our previous work [17], we presented the design of a PNSA. In this paper, we, first, outline the theoretical foundation of the new class of PNSAs, and second, we present a detailed modeling, analysis, and experimental characterization of a prototype positive-negative stiffness actuator. The proposed actuation concept extends our previous work on low-power stiffness modulation [18]–[21] in an unexpected way by introducing effectively tunable negative stiffness as a novel means of actuation.

In Section II, we present a brief review of the mathematical design conditions that characterize SEAs and VSAs. Section III introduces the class of PNSAs. This section contains a set of analytical conditions that can be used to define, identify, or design PNSAs. A prototype PNSA is presented in Section IV, together with its mathematical model and experiential characterization. Finally, in Section V, we present experimental data demonstrating wide-range stiffness and equilibrium position modulation achievable with the proposed PNSA.

II. Compliant Actuators

Variable stiffness actuators and series elastic actuators are typical positive stiffness actuators. In this section, we revisit the main design features of these positive stiffness actuators, including the means by which they enable equilibrium position and stiffness modulation. This analysis leads to a new class of compliant actuators which provide, first, *design simplification* compared to previously designed VSAs, and second, intrinsically stable *open-loop stiffness modulation* unlike similarly complex SEAs.

A. Variable Stiffness Actuators

Variable stiffness actuators [23]–[32] employ an elastic element (spring) to couple the position at the actuator's output q with two motor positions $\mathbf{q}_m = [q_{m\,1}, q_{m\,2}]^\top$ at the actuator's input, see Fig. 1. Although, VSAs could be designed differently, all of them can be represented by a unified mathematical model. In this paper, we present and analyze this unified model.

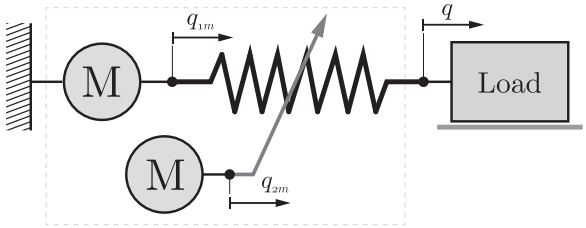

Fig. 1. Minimalistic model of a VSA. In this model, q is the output position while $\mathbf{q}_m = [q_{m\,1}, q_{m\,2}]^\top$ are the motor positions.

The dynamics of the actuator's output and the closed-loop dynamics of the motor position inputs are given by the following two equations:

$$\ddot{q} + \beta\dot{q} = f_a(q, \mathbf{q}_m), \tag{1}$$

$$\ddot{\mathbf{q}}_m + 2\alpha\dot{\mathbf{q}}_m + \alpha^2\mathbf{q}_m = \alpha^2\mathbf{u}(t) \tag{2}$$

where $\beta > 0$ is the damping at the output, $f_a(q, \mathbf{q}_m)$ is the force at the output, $\alpha > 0$ defines the closed-loop bandwidth of the motor dynamics while $\mathbf{u} = [u_1, u_2]^\top$ are the control inputs.

Using the control inputs one can change the motor positions. This may be best illustrated by noting that $\mathbf{q}_m = \mathbf{u}$ under steady-state conditions. Also, by changing the motor positions $\mathbf{q}_m$ one can modulate the output equilibrium position

$$q^* = q^*(\mathbf{q}_m) \in \{q^* \in \mathbb{R} : f_a(q^*, \mathbf{q}_m) = 0, \mathbf{q}_m \in \mathbb{R}^2\} \tag{3}$$

under the following analytical design condition:

$$\frac{\partial f_a(q^*, \mathbf{q}_m)}{\partial \mathbf{q}_m} \neq \mathbf{0}.$$

According to the implicit function theorem [33], *existence* of an equilibrium necessitates $\partial f_a(q, \mathbf{q}_m)/\partial q|_{q=q^*(\mathbf{q}_m)} \neq 0$, while *uniqueness* and *stability* of the equilibrium requires that the actuator is characterized by a restoring force–deflection relation for any fixed motor position, i.e., $f_a(q^* + \delta q, \mathbf{q}_m) \approx -k_a(q^*, \mathbf{q}_m)\delta q$, where the stiffness is *strictly positive*

$$k_a(q^*, \mathbf{q}_m) = -\frac{\partial f_a(q, \mathbf{q}_m)}{\partial q}\Big|_{q=q^*(\mathbf{q}_m)} > 0. \tag{4}$$

The above definition (3) suggests that it may be possible to have the same output equilibrium position using different motor positions. This requires the following linear equation to have nontrivial solutions:

$$f_a(q^*, \mathbf{q}_m^* + \delta\mathbf{q}_m) \approx \frac{\partial f_a(q^*, \mathbf{q}_m)}{\partial \mathbf{q}_m}\Big|_{\mathbf{q}_m = \mathbf{q}_m^*} \delta\mathbf{q}_m = 0.$$

Existence of the nontrivial solution is assured under the following analytical condition:

$$\mathbf{I}_{2\times 2} - \left[\frac{\partial f_a}{\partial \mathbf{q}_m}\right]^+ \left[\frac{\partial f_a}{\partial \mathbf{q}_m}\right] \neq \mathbf{0}. \tag{5}$$

This is only a necessary condition to change the stiffness independent of the equilibrium position. Indeed, modulation of the stiffness using the motor positions, $\delta k_a(q^*, \mathbf{q}_m + \delta\mathbf{q}_m) \approx [\partial k_a(q^*, \mathbf{q}_m)/\partial \mathbf{q}_m]\delta\mathbf{q}_m$, requires $\partial k_a(q^*, \mathbf{q}_m)/\partial \mathbf{q}_m \neq \mathbf{0}$. As such, independent control of the stiffness and the equilibrium

position can only be assured by the following sufficient condition[1] [7]:

$$\left(\frac{\partial k_a}{\partial \mathbf{q}_m}\right)\left(\mathbf{I}_{2\times 2} - \left[\frac{\partial f_a}{\partial \mathbf{q}_m}\right]^{+}\left[\frac{\partial f_a}{\partial \mathbf{q}_m}\right]\right) \neq \mathbf{0}. \tag{6}$$

One of the simplest models that is consistent with the above conditions is defined by the following relation:

$$f_a(q, \mathbf{q}_m) = -(k_0 + k_1 q_{2m})(q - q_{1m}). \tag{7}$$

In this model, the equilibrium position is directly defined by the first motor, i.e., q_{1m}, while the stiffness at the equilibrium is controllable by the second motor q_{2m}

$$q^* = q_{1m} \quad \text{and} \quad k_a(q_{2m}) = k_0 + k_1 q_{2m}. \tag{8}$$

Given a unit step input

$$\mathbf{u}(t) = 1(t)[q_d^*, (k_d^* - k_0)/k_1]^{\top} \tag{9}$$

(where q_{d}^* is the desired equilibrium and k_{d}^* is the desired stiffness), the equilibrium position and the stiffness change in the following way:

$$q^*(t) = q_d^* - (1 + \alpha t)\mathrm{e}^{-\alpha t} q_d^*$$
$$k_a(t) = k_d^* - (1 + \alpha t)\mathrm{e}^{-\alpha t}(k_d^* - k_0).$$

According to (8), the equilibrium position and the stiffness algebraically depend on the motor positions and as such control over these two modalities can be realized without using feedback from the output position, see (9). In order to achieve this, VSAs require (at least) two independent motor inputs as implied by (5). However, two motors make these actuators more complex, larger, and heavier, compared to actuators that require only one motor. Also, the introduction of the second motor could increase the energy required by the actuator.

In many practical applications, it may be desirable to eliminate one of the motors, to reduce the complexity of VSAs, but without giving up the ability to control both the stiffness and the equilibrium position. One way to do this is to employ closed-loop control using a simpler SEA.

B. Series Elastic Actuators

Series elastic actuators [3] permit a simpler design realization compared to VSAs, see Fig. 2. The closed-loop behavior of SEAs can be understood using the following model:

$$\ddot{q} + \beta \dot{q} = f_a(q, q_m), \tag{10}$$

$$\ddot{q}_m + 2\alpha \dot{q}_m + \alpha^2 q_m = \alpha^2 u(t, q) \tag{11}$$

where the first equation describes the dynamics at the output while the second equation represents the closed-loop dynamics of the motor. Compared to VSAs (1) and (2), here, there is only one motor position input q_m, which can be used for open-loop control of a unique and stable $\partial f_a(q, q_m)/\partial q|_{q=q^*(q_m)} > 0$ equilibrium position

$$q^* = q^*(q_m) \in \{q^* \in \mathbb{R} : f_a(q^*, q_m) = 0, q_m \in \mathbb{R}\}$$

given the following design condition: $\partial f_a(q^*, q_m)/\partial q_m \neq 0$. However, unlike the stiffness of an open-loop controlled VSA (4), the stiffness of a closed-loop controlled SEA is given by the following relation:

$$k_a(q^*, q_m) = \underbrace{-\frac{\partial f_a(q, q_m)}{\partial q}\Big|_{q=q^*}}_{k_a^{\mathrm{OL}}} \underbrace{-\frac{\partial f_a(q^*, q_m)}{\partial q_m}\frac{\partial q_m}{\partial q}}_{k_a^{\mathrm{CL}}} \tag{12}$$

where the first term represents the open-loop stiffness k_a^{OL}, while second term is the closed-loop stiffness k_a^{CL}.

For a given equilibrium position q^*, the motor position q_m and the open-loop stiffness k_a^{OL} are both fixed for any single valued, linear or nonlinear, function $f_a(q, q_m)$. Consequently, the apparent output stiffness of the actuator can only be changed through the second term in (12) if output position feedback is present in the control law $u = u(t, q)$. This assertion may be best exemplified by noting that $\partial q_m/\partial q = \partial u(t, q)/\partial q$ in a steady-state condition. Accordingly, modulating the output position gain in the control law—$\partial u/\partial q$—by software control can be used to modulate the output stiffness of the actuator.

A minimalistic model of a SEA (see Fig. 2), and the simplest control law[2] set to achieve a desired equilibrium position and stiffness, are given by:

$$f_a(q, q_m) = -k_0(q - q_m), \tag{13}$$

$$u(t, q) = q - k_0^{-1} 1(t) k_d^*(q - 1(t) q_d^*). \tag{14}$$

Just like in VSAs (7), the equilibrium position here is defined by the motor positions (13), but unlike in VSAs, the stiffness at the equilibrium now depends on the control law (14). Despite this difference, the equilibrium position and the stiffness can be controlled in the very same way as on the previously discussed VSA:

$$q^*(t) = q_d^* - (1 + \alpha t)\mathrm{e}^{-\alpha t} q_d^*,$$
$$k_a(t) = k_d^* - (1 + \alpha t)\mathrm{e}^{-\alpha t}(k_d^* - k_0).$$

According to these relations, it appears that there is no difference between SEAs and VSAs when it comes to equilibrium position and stiffness modulation. This assertion is however misleading. The reason is that the introduction of output feedback in the

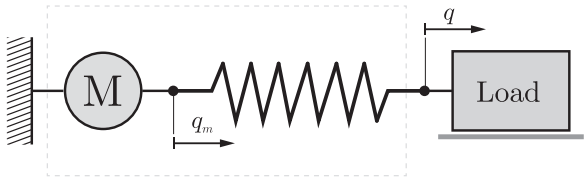

Fig. 2. Minimalistic model of a SEA. In this model, q is the output position while q_m is the motor position.

[1]It may be shown that a typical antagonistic actuator equipped with two motor units and two linear springs satisfies the above-mentioned necessary condition (5), but does not satisfy the sufficiency condition (6) because it does not provide control over the output stiffness. It can be also shown that the same actuator equipped with nonlinear springs having quadratic force–displacement characteristic does satisfy the sufficiency condition (6) and is known to allow independent control over the stiffness and the equilibrium position [27].

[2]This is the "simple impedance controller" proposed by Hogan [2].

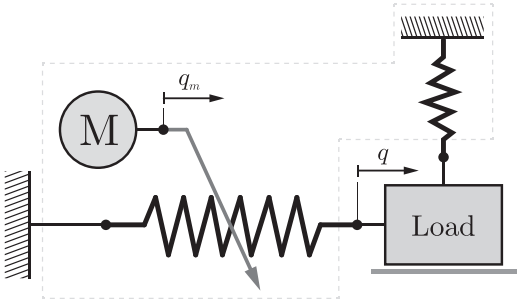

Fig. 3. Minimalistic model of a PNSA. In this model, q is the output position while q_m is the motor position.

control law (14) makes SEAs vulnerable to instability [10], [34]. This may be best exemplified by noting that a desired stiffness k_d^* that can be stably realized on SEAs must obey the following condition:

$$0 < k_d^* \leq \frac{(\alpha\beta + 2k_0)(2\alpha(\alpha+\beta)^2 + \beta k_0)}{\alpha(2\alpha+\beta)^2} \tag{15}$$

in case of an interaction-free manipulation, and

$$0 < k_d^* \leq k_0 + \frac{1}{2}\alpha\beta \tag{16}$$

when the output is in contact with a passive environment. The first condition (15) is required to ensure stability when the system does not interact with the environment—for example, during the swing phase in locomotion assisted by prosthetic limb driven by a SEA—while the second condition (16) is required to ensures that the system does not go unstable while interacting with a passive environment—for example, during the stance phase in locomotion. If the former condition is not respected then the desired stiffness k_d^* will not be achieved. If the latter condition is not respected then the actuator could become unstable upon interaction with a passive environment. Although there are sophisticated controllers that can extend the stiffness modulation capabilities of SEAs, they are subject to similar stiffness range limitations. Thus, due to the output feedback in the control law, the desired stiffness is limited if the stability of the closed-loop system is to be preserved.

Performing an inherently stable open-loop stiffness modulation, similar to VSAs, using a single motor unit, similar to SEAs, may be desirable in practical applications. In the following, we present a novel actuator that may comply with these requirements.

III. Positive–Negative Stiffness Actuators

We propose a new type of PNSA with the aim to achieve both equilibrium position control and stiffness modulation using a single motor and without closed-loop output position control. A schematic representation of this actuator is depicted in Fig. 3.

The mathematical model of the actuator is given by:

$$\ddot{q} + \beta\dot{q} = f_a(q, q_m),$$
$$\ddot{q}_m + 2\alpha\dot{q}_m + \alpha^2 q_m = \alpha^2 u(t).$$

Compared to VSAs, (1) and (2), there is only one motor here q_m while compared to SEAs, (10) and (11), the controller does not involve feedback from the output position. On positive-stiffness SEAs these features imply that only the equilibrium position can be controlled. On the contrary, PNSAs have one equilibrium position q_0^* at which the stiffness is also controllable. This added feature necessitates the following analytical conditions:

$$\exists q^* = q_0^* \text{ such that } \forall q_m : \text{C.1} \quad f_a(q_0^*, q_m) = 0,$$
$$\text{C.2} \quad \frac{\partial k_a(q_0^*, q_m)}{\partial q_m} > 0.$$

The first condition defines the trivial equilibrium position q_0^* and indicates independence of the output force from the motor position. The second condition asserts controllable stiffness at the equilibrium position q_0^*. This second condition also implies that the stiffness is a monotonically increasing function of the motor position.[3]

Control over an equilibrium position, e.g., q_0^*, is not possible if the actuator is stable at that particular position. However, control over q_0^* may be achieved if the actuator is made unstable at that position. This requires the following equation to have nontrivial solutions:

$$f_a(q_0^* + \delta q, q_m^*) \approx -k_a(q_0^*, q_m^*)\delta q + \frac{1}{6}\frac{\partial^3 f_a(q_0^*, q_m^*)}{\partial q^3}\delta q^3 = 0.$$

Existence of a nontrivial solution to the above equation asserts two new analytical conditions:

$$\text{C.3} \quad \exists q_{m0} \text{ such that } \forall q_m < q_{m0} : \quad k_a(q_0^*, q_m) < 0,$$
$$\text{C.4} \quad \forall q_m < q_{m0} : \quad \frac{\partial^3 f_a(q_0^*, q_m)}{\partial q^3} < 0.$$

The former condition means that the actuator has *negative stiffness* at the natural equilibrium position q_0^* for a certain range of motor positions, while the latter condition implies that the actuator has a *softening nonlinear force–deflection characteristic* for the same range of motor positions.

Under the above conditions, i.e., C.1–C.4, there are two distinct operation modes of the actuator: 1) when the stiffness is positive $k_a(q_0^*, q_m > q_{m0}) > 0$ the actuator has a single stable equilibrium position q_0^* and 2) when the stiffness is negative $k_a(q_0^*, q_m < q_{m0}) < 0$ the actuator has three equilibrium positions.[4] These are the natural equilibrium at q_0^*, which is now *unstable*, and two new equilibriums, which are stable:

$$q_\pm^* = q_0^* \pm \sqrt{6}\left[\left(\frac{\partial^3 f_a(q_0^*, q_m^*)}{\partial q^3}\right)^{-1} k_a(q_0^*, q_m^*)\right]^{\frac{1}{2}}.$$

Given that the stiffness is a continuous function of the motor position, the nontrivial equilibrium positions are also continuous

[3]With no restriction on generality, we may also assume that the stiffness is a monotonically decreasing function of the motor position. This is because, by changing the assumed positive direction of the motor position q_m one can convert a monotonically decreasing stiffness function to an equivalent monotonically increasing one.

[4]When the stiffness is zero $k_a(q_0^*, q_m = q_{m0}) = 0$, the actuator goes through bifurcation, which is a transition between the above mentioned two qualitatively different operation modes.

with respect to the motor position. This shows controllability of the nontrivial equilibrium positions $q^*_\pm$ using the motor position q_m.

In order to demonstrate the working principle of a PNSA, we will now consider a minimalistic model

$$f_a(q, q_m) = -(k_0 + k_1 q_m)q + k_3 q^3$$

where $k_0 < 0$ represents the *negative stiffness*, $k_1 q_m$ denotes the controllable positive stiffness ($k_1 > 0$) while $k_3 < 0$ represents the *softening nonlinearity*. The nonlinear term is typical, it resembles the odd symmetry in a general passive force–deflection relation $f_a(q, q_m) = -f_a(-q, q_m)$.

Based on the above model, the actuator has the following two distinct modes of operation:

I) When the stiffness at the origin ($q = 0$) is positive, the actuator has a stable trivial equilibrium position ($q^*_0 = 0$). At this equilibrium position, the stiffness can be changed by varying the motor position:

$$\forall q_m \geq q_{m0} = -k_0/k_1 : \begin{cases} q^* = q^*_0 = 0 \\ k_a(0, q_m) = k_0 + k_1 q_m . \end{cases}$$

II) When the stiffness at the origin is negative, the actuator has two nontrivial equilibrium positions, which can be controlled using the motor position:

$$\forall q_m < q_{m0} = -k_0/k_1 :$$

$$\begin{cases} q^*_\pm(q_m) = \pm \left[\dfrac{k_0 + k_1 q_m}{k_3} \right]^{\frac{1}{2}} \\ k_a(q, q_m) = k_0 + k_1 q_m + 3k_3 q^2 . \end{cases}$$

Thus, depending on the motor position q_m, the actuator could be in the I) stiffness modulation mode at the trivial equilibrium position $q^*_0 = 0$, or in the II) equilibrium control mode at one of its nontrivial equilibria $q^*_\pm \neq 0$. In the latter case, preference toward a particular equilibrium position, e.g., $q^*_+ > 0$, can be ensured by introducing a small "design imperfection" that deliberately breaks the perfect symmetry assumption, i.e., $f_a(q, q_m) \approx -f_a(-q, q_m)$ [35]. Alternatively, the nontrivial solution can also be made unique by designing a *unilateral actuator*, i.e., $q \geq 0$. In the next section, we use both of these features to present a compliant unilateral robot knee joint that employs positive–negative stiffness actuation.

IV. Realization of the PNSA

The analytical conditions, C.1–C.4, listed in the previous section, represent a set of conditions for the design of PNSAs. However, these conditions do not provide a guideline to design one such actuator. Nevertheless, the idea to design PNSAs is relatively simple, namely one can use a controllable positive stiffness system in conjunction with a passive negative stiffness system, connected in parallel to the same output link.

Figure 4(a) shows one such realization where a variable length positive stiffness leaf-spring mechanism (see Fig. 4(b) blue and green) is connected in parallel with a passive negative stiffness compression spring mechanism, see Fig. 4(b) red.

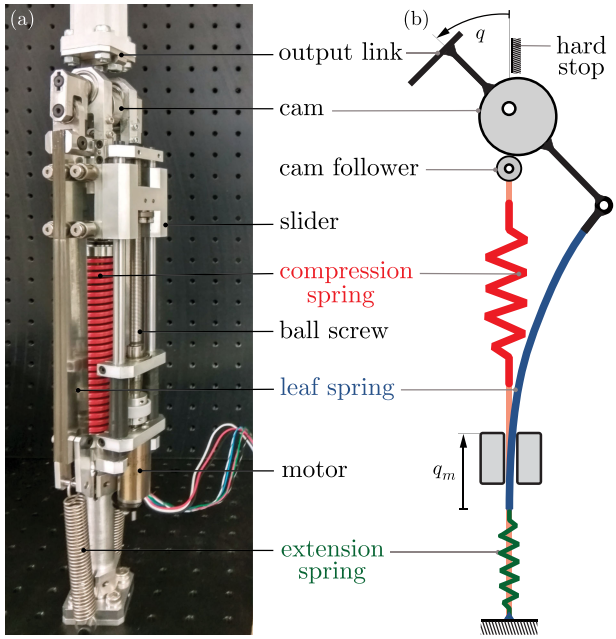

Fig. 4. Positive–negative stiffness actuator. (a) Hardware implementation. (b) Schematic representation.

The design, characterization, and the working principle of the two separate mechanisms, and the composite mechanism, are detailed in Sections IV-A, IV-B, and IV-C.

A. Positive Stiffness Mechanism

The positive stiffness mechanism (see Fig. 5(a)) is a modified version of our previous design [18]. The main component of this mechanism is a variable-length leaf-spring shown in Fig. 5(a). This mechanism is composed of an output link OA, a rigid connector link AB, a leaf-spring (blue) and a position controlled slider. The leaf spring is rigidly connected to the connector link at point B and is attached to the extension spring (green) at the other end. The modification with respect to our previous design concerns the green extension spring. This extension spring is used to tune the passive force–deflection characteristic of the device; it extends the positive stiffness operation range of this design.

Using the Bernoulli–Euler beam theory [36], the nonlinear model of the positive stiffness mechanism is given by the following equations:

$$L = \sqrt{\frac{EI}{2}} \int_0^{\theta_L} \frac{d\theta}{\sqrt{f(M_L, F_y, F_x, \theta, \theta_L)}}, \tag{17}$$

$$x_L = \sqrt{\frac{EI}{2}} \int_0^{\theta_L} \frac{\cos(\theta) d\theta}{\sqrt{f(M_L, F_y, F_x, \theta, \theta_L)}}, \tag{18}$$

$$y_L = \sqrt{\frac{EI}{2}} \int_0^{\theta_L} \frac{\sin(\theta) d\theta}{\sqrt{f(M_L, F_y, F_x, \theta, \theta_L)}} \tag{19}$$

where L is the active length of the deformed leaf-spring, (x_L, y_L) denotes the end point B of the leaf-spring, θ_L is the deflection angle at point B while $f = \frac{M_L^2}{2EI} + F_y[\sin(\theta_L) -$

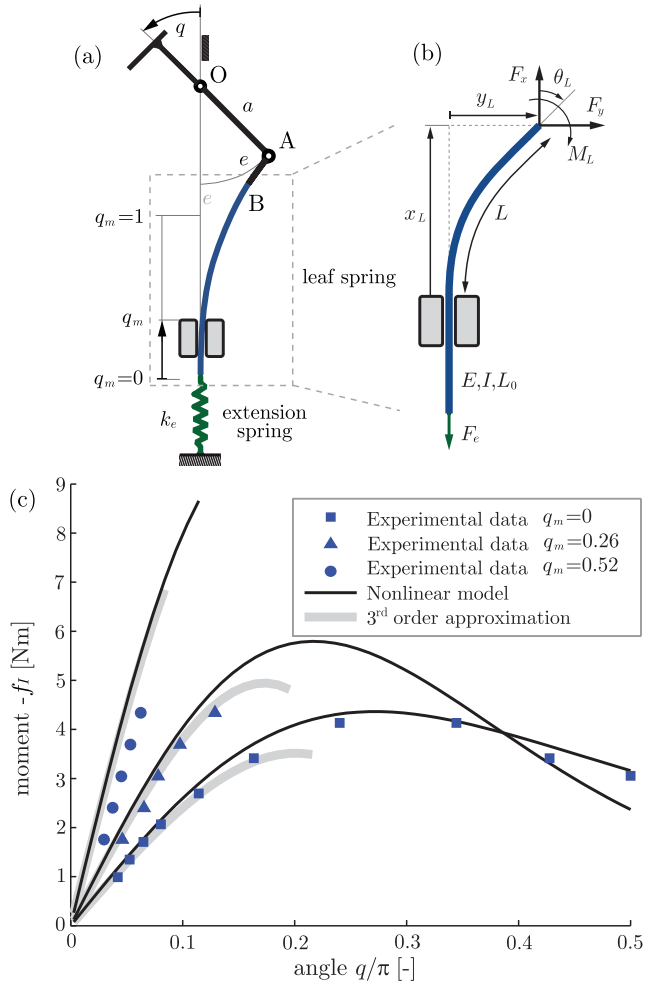

Fig. 5. (a) Positive-stiffness mechanism composed of leaf-springs and extension springs. (b) Details of the leaf-spring design. The prototype employs two stacks of 20 mm wide and 10 mm thick leaf-springs. These springs are made of 1 mm and 0.5 mm thick spring steel plates. The effective length of these plates is $L_0 = 77$ mm. The total area moment of inertia of the leaf-spring stack is $I = 11.6 \times 10^{-12}$ m^4. The Young modulus of the spring steel material is $E = 200 \times 10^9$ N/m^2. There are also two extension springs (green) in this design. The stiffness of these two springs is $k_e = 1360$ N/m. These springs are pre-extended by $F_{e0} \approx 70$ N force. (c) Moment–deflection relation. The predictions of the nonlinear model are shown with solid black lines. The predictions of the approximate analytical model are shown with gray lines. The experimental data are shown with blue markers.

$\sin(\theta)] + F_x[\cos(\theta_L) - \cos(\theta)]$ and $M_L = eF_y \cos(\theta_L) - eF_x \sin(\theta_L)$ where F_x, F_y, and M_L denote the reaction forces and the reaction moment at point B, E is Young's modulus and I is the area moment of inertia of the spring, see Fig. 5(b).

In addition to (17)–(19), the following geometric constraints are present in the proposed design:

$$\begin{aligned} x_L &= L_0(1 - q_m) + a(1 - \cos q) + e(1 - \cos\theta_L), \\ y_L &= a \sin q - e \sin\theta_L \end{aligned} \tag{20}$$

where q is the link angle, q_m is the dimensionless slider position, L_0 is the total length of the leaf-spring while $a = $ OA and $e = $ AB are the lengths of the lever arms shown in Fig. 5(a).

Finally the static force experienced by the motor F_m is defined by the following equation [37]:

$$F_m = \frac{(M_L + F_y x_L - F_x y_L)^2}{2EI} = F_e - F_x \tag{21}$$

where $F_e = F_{e0} + k_e(L + a(1 - \cos q) - x_L)$ is the force generated by the extension spring attached to the free end of the leaf spring. In the latter relation, k_e is the spring stiffness while F_{e0} is the force used to pretension the spring.

Using (17)–(21) one can numerically compute the output torque of the positive-stiffness mechanism as a function of the link angle q and the motor position q_m

$$f_{\rm I}(q, q_m) = -F_y(q, q_m)a \cos q - F_x(q, q_m)a \sin q.$$

The numerically computed torque–deflection curves are shown in Fig. 5(c) (black lines) for different values of the motor position. Comparison with the experimental data (see Fig. 5(c) blue markers) shows the predictive power of the nonlinear model.

Assuming small deformations, an approximate analytical model of the same torque–deflection relation is given by

$$f_{\rm I}(q, q_m) \approx -k_{\rm I1}(q_m)q + k_{\rm I3}(q_m)q^3 \tag{22}$$

where $k_{\rm I1}(q_m)$ is given in (23) while $k_{\rm I3}(q_m)$ is given in the Appendix. This expression provides a reasonably good approximation of the experimental data near to the trivial equilibrium of the positive stiffness mechanism (see Fig. 5(c) gray lines).

The stiffness of this mechanism

$$k_{\rm I1}(q_m) = aF_{e0} + \frac{3EI}{L_0} \frac{\left(\frac{a}{L_0}\right)^2}{\left(1 + \frac{e}{L_0} - q_m\right)^3 - \left(\frac{e}{L_0}\right)^3} \tag{23}$$

is positive and approaches infinity as the active length of the leaf-spring approaches zero ($q_m \to 1$). We will subsequently describe the negative stiffness mechanism, which has qualitatively different properties.

B. Negative Stiffness Mechanism

The negative stiffness mechanism (see Fig. 6) is composed of a compression spring (red) and a roller cam mechanism (gray). The moment produced by the spring is zero for zero output deflection while it is positive for positive output deflections. Upon deflection the spring tends to push the output away from the origin. This creates instability at the trivial equilibrium position ($q = 0$).

The cam is circular with radius R, but it is eccentrically mounted on the output shaft. The cam profile is given by

$$\rho(\theta, q) = \frac{1}{8}R\left[5\cos(\theta - q) + \sqrt{64 - 25\sin^2(\theta - q)}\right] \tag{24}$$

where ρ is the polar radius measured from the axis of rotation of the cam, and $\theta \in [0, 2\pi]$ is the polar angle measured from the axis that connects the centers of the cam and the center of the cam follower, see Fig. 6(b).

The moment produced by the mechanism at the output link is a function of the cam profile (24), the cam-follower radius r, and the angle of contact between the cam and the cam follower

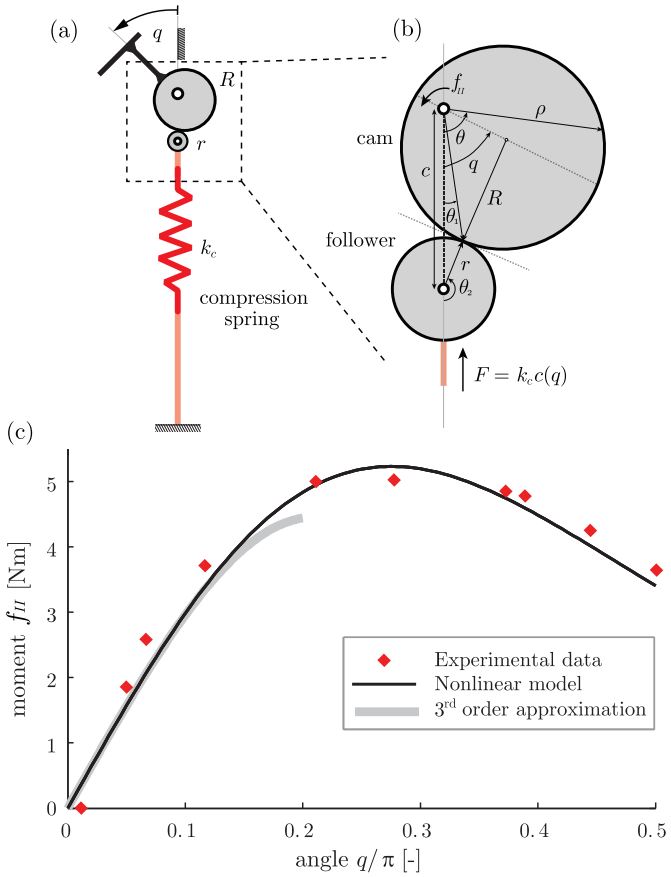

Fig. 6. (a) Cam-compression spring mechanism. (b) Details of the cam design. (c) Moment–deflection characteristic of the mechanism. The physical parameters of the mechanisms are given by the radius of the cam $R = 0.016$ m, the radius of the cam follower $r = 0.006$ m, and the stiffness of the compression spring $k_c = 21\,900$ N/m.

θ_2, see Fig. 6(b). The exact moment–deflection characteristic of this mechanism is obtained by solving the following equations:

$$\begin{aligned} &\rho(\theta_1, q)\sin(\theta_1) - r\sin(\theta_2) = 0,\\ &\rho(\theta_1, q)\cos(\theta_1) - r\cos(\theta_2) - c(q) = 0,\\ &s(\theta_1, q) - \tan(\theta_2) = 0 \end{aligned} \tag{25}$$

where $c(q)$ is the distance between the centers of the cam and the cam follower, while

$$s(\theta_1, q) = \left.\frac{\frac{d\rho}{d\theta}\sin\theta + \rho\cos\theta}{\frac{d\rho}{d\theta}\cos\theta - \rho\sin\theta}\right|_{\theta=\theta_1}$$

is the slope of the tangent line to the cam surface at the point of contact between the cam and the cam follower, see Fig. 6(b). In our design, $c(q)$ represents the compression of the spring. Consequently, the moment generated by the spring at the output is given by:

$$f_{II}(q) = \frac{1}{2}k_c c(q)^2 \sin(2\theta_2(q))$$

where k_c is the stiffness of the compression spring. The numerically computed torque–deflection curve and the corresponding experimental data are shown in Fig. 6(c).

The approximate analytical relation between the moment produced by the spring and the output angle is

$$\begin{aligned} f_{II}(q) &\approx -k_{II1}q + k_{II3}q^3\\ &= \frac{5}{512}k_c R^2 \frac{(13+8\frac{r}{R})^2}{(1+\frac{r}{R})}q\\ &\quad - \frac{1895}{196608}k_c R^2 \frac{(13+8\frac{r}{R})^2}{(1+\frac{r}{R})^3}\left[1 + \frac{368}{379}\frac{r}{R} + \frac{64}{379}\frac{r^2}{R^2}\right]q^3. \end{aligned} \tag{26}$$

This expression provides a reasonably good approximation of the experimental data near to the origin, see Fig. 6(c). The stiffness of the mechanism at the trivial equilibrium is given by

$$k_{II1} = -\frac{5}{512}k_c R^2 \frac{(13+8\frac{r}{R})^2}{(1+\frac{r}{R})}. \tag{27}$$

As can be seen this stiffness is always negative.

In the following, we aim to use the analytical expressions derived in this section in order to better understand the behavior of the proposed PNSA.

C. Positive-Negative Stiffness Actuator

The previously described two mechanisms are connected in parallel, and they act against each other at the output link. Similar to helical springs connected in parallel, the overall force–deflection relation of the resulting composite mechanism is the sum of force–deflection relations of the two individual mechanisms, (22) and (26):

$$f_a(q, q_m) = f_I(q, q_m) + f_{II}(q).$$

The resulting PNSA has the following features:

C.1) The undeflected configuration is the equilibrium position of the actuator, irrespective of the motor position:

$$\forall q_m \in [0,1] : f_a(0, q_m) = 0.$$

As a direct implication, at the trivial equilibrium position, the output force cannot be changed by changing the motor position.

C.2) The stiffness of the actuator at the origin is a monotonically increasing function of the motor position:

$$\begin{aligned} \forall q_m \in [0,1] : \frac{\partial k_a(0,q_m)}{\partial q_m} &= \frac{\partial k_{I1}(q_m)}{\partial q_m} + \frac{\partial k_{II1}}{\partial q_m}\\ &= \frac{9EI}{L_0}\left(\frac{\left(\frac{a}{L_0}\right)\left(1+\frac{e}{L_0}-q_m\right)}{\left(1+\frac{e}{L_0}-q_m\right)^3 - \left(\frac{e}{L_0}\right)^3}\right)^2 > 0. \end{aligned} \tag{28}$$

C.3) At the origin, the stiffness of the actuator can take negative values for a range of motor positions:

$$\forall q_m \in [0, q_{m0}) : k_a(0, q_m) = k_{I1}(q_m) + k_{II1} < 0$$

where

$$q_{m0} = 1 + \frac{e}{L_0} - \left(\left(\frac{e}{L_0} \right)^3 - \frac{3EI}{L_0} \frac{\left(\frac{a}{L_0} \right)^2}{aF_{e0} + k_{\text{II}1}} \right)^{\frac{1}{3}} < 1$$

given that the pretension of the extension spring is not too large $aF_{e0} + k_{\text{II}1} < 0$, where $k_{\text{II}1} < 0$, see (27).

C.4) The force–deflection characteristic near to the origin is described by a softening nonlinear relation:

$$\forall q_m \in [0, q_{m0}) :$$

$$\frac{\partial^3 f_a(q, q_m)}{\partial q^3}\Big|_{q=0} = 6(k_{\text{I}3}(q_m) + k_{\text{II}3}) < 0.$$

The actuator has a number of added features that set it apart from more typical previously designed compliant actuators. These features are listed as follows.

C.5) The actuator has unprecedented stiffness tunability, i.e., the minimum stiffness can be negative while the maximum stiffness can theoretically reach positive infinity

$$q_m \in [0, 1] : k_a(0, q_m) = k_{\text{I}1}(q_m) + k_{\text{II}1} \in [-1.9, \infty).$$

This stiffness range goes beyond the ranges reported for previously designed VSAs, which may have infinite but only-positive stiffness capability [29], [30], [32]. Also, a typical stiffness modulator, used in number of previously designed actuators, has a finite positive stiffness range [28], [31], [38], [39].

C.6) The actuator employs a passive negative stiffness mechanism. This means that no energy is required to generate negative stiffness. This feature makes our implementation energetically advantageous compared to designs that require active control, and as such energy input, to generate or change the negative stiffness [11]–[14]. In order to substantiate this point, we note that buckling-beam-based negative stiffness systems are characterized by an approximate linear relation between the axial compression force F_m, provided by the motor or piezoelectric actuator, and the lateral stiffness of the beam k_a at equilibrium [12]:

$$\forall k_a \in \mathbb{R}, q = 0 : \frac{F_m}{F_{cr}} \approx 1 - \frac{k_a}{k_0}$$

where F_{cr} is the critical buckling force, and k_0 is the lateral stiffness of the beam when no motor force is applied $F_m = 0$. According to this relation, first, holding stiffness requires nonzero motor force, just like in antagonistic actuators [26], and second, negative stiffness $k_a \leq 0$ requires a motor force that is larger than the critical buckling force $F_m \geq F_{\text{cr}}$. Even if a large motor force could be supported by a nonbackdrivable mechanism (lead screw or clutch) inserted in the load path, changing stiffness would still require the motor to provide this force. This means high motor force and high energy cost. In contrast, the motor force is zero and *independent of the stiffness at equilibrium* in the proposed PNSA:

$$\forall k_a \in \mathbb{R}, q = 0 : \; F_m = 0.$$

This means smaller motor force and lower energy cost.

C.7) The leaf-spring used in the actuator requires intrinsically low motor force for stiffness modulation [18]. This is because the variable length leaf-spring design belongs to the class of mechanisms that require finite static motor force irrespective of the output position and output stiffness [19], [20].

C.8) The actuator has an 81% efficient drive train according to factory specifications; it consist of a 90% efficient DC motor coupled to a 90% efficient ball screw without using any additional gearbox. This was made possible by the geometric design of the leaf-spring mechanism, which displaces the motor from the load path. As an implication, the motor force required for stiffness modulation can be kept low [20], compared to an alternative antagonistic [26], [40] or spring pretension-based actuator [8], [28], [38].

C.9) The actuator has a reasonably large but limited motion range. This has been achieved by the kinematic connection of the leaf-spring element and the output link (see Fig. 5(a) OAB). This connection limits the deformation of the leaf under large deflections of the actuator. Further to this, with the use of the extension springs (see Fig. 5(a) green), the variable-length leaf spring mechanism possesses an extended positive stiffness range for large deflections compared to the design in [18].

C.10) The actuator uses a nonlinear phenomenon, bifurcation, to switch between equilibrium position control and stiffness modulation using a single motor. This design differs from previous designs that use a controllable clutch to emulate similar functionality [22], [23]. While the idea to use a controllable clutch is appealing, the technical realization of this idea remains challenging. In particular, designing a clutch that can switch between equilibrium position control and stiffness modulation can be more complex than the classical design that uses two motors. In the proposed actuator, we replace one of the motors with a *relatively simple* compression spring mechanism, see Fig. 6(a). Further simplification may be possible using algorithmic design exploration [41].

The analytical model derived in this section provides a reasonably good approximate representation of the actuator near to its trivial equilibrium position $q \approx 0$. However, this model is not general enough to predict the location of the nontrivial equilibrium away from the zero position. For this reason, we now resort to an experimental characterization of the proposed PNSA.

V. Experiments

In this section, we use the proposed PNSA to emulate the behavior of the biological knee joint during locomotion. There are two distinct motion phases—stance phase and swing phase—during human locomotion. In the stance phase, the knee contributes to weight bearing of the body while maintaining a stiff and nearly straight configuration of the lower limb. In the swing phase, the function of the knee joint changes because it requires control over the joint equilibrium position to generate the flexion (early swing) and extension (late swing) [42]. Thus, locomotion necessitates the knee to have two distinct modes of operation, first, relatively high stiffness near to the zero equilibrium position during the stance phase, and second, equilibrium position control with lower stiffness in the swing phase. Through the following two experiments we aim to show how can the proposed device emulate similar operational features.

A. Stiffness Control Mode

In the first experiment, we demonstrate the effect of stiffness modulation for a weight-bearing task without allowing for significant deflection of the joint. This is similar to the function of the knee joint during the stance phase [43]. In the remainder of this section, we consider this to be a stabilization task.

Figure 7 shows the experimental setup for the stabilization task. Here, the device is secured to the floor while having a weight on the top. This inverted pendulum setup is similar to the stance phase in locomotion where the foot is in contact with the ground and the leg supports the upper body. The effective output stiffness is quantified using a constant additional moment, i.e., provided by a second weight attached to the output link through a pulley. Starting from a slightly deflected configuration ($q_m = 0.58$) see Fig. 7(a-i), the slider was gradually moved toward higher stiffness settings ($q_m = 0.78$). This made the joint angle approach zero $q \approx 0$, see Fig. 7(a-ii). Subsequently, the slider was moved back to its initial position ($q_m = 0.58$), and consequently, the joint returned to a deflected position, see Fig. 7(a-iii). During this experiment, the position of the slider and the output deflection of the joint were recorded, and the stiffness of the joint was calculated according to the following approximate relation[5]: $k(0, q_m) \approx M/q$, where M is the net moment generated by the upper part of the setup and the weight attached to the output link.

As the slider reduces the active length of the leaf-spring, ($q_m \to 0.78$) see Fig. 7(b), the stiffness varies at higher rate, see Fig. 7(c), thereby allowing for a faster modulation between a rigid and a compliant behavior. This can be attributed to the approximate inverse cubic relation between the stiffness and the motor position, i.e., $k_a(0, q_m) \propto (1 - q_m)^{-3}$, according to (28). However, unlike predicted by the model, it is not possible to achieve infinite stiffness on the actuator even if ($q_m \to 1$). This limitation is fundamental on real-world devices affected by material yielding and design imperfection, e.g., backlash at the zero equilibrium position. Also, determining the largest stiffness experimentally is challenging because at high stiffness sensory noise and small changes in the motor position can result in significant changes in the stiffness values (see Fig. 7(c) error bars). Despite these effects, if high stiffness is desired, the output link may be *kinematically locked* by moving the slider into the rigid connector link AB, see Fig. 5(a). In such case, the output stiffness becomes the structural stiffness of the actuator. Finally, we note that the electrical power consumption of the motor was low in this experiment, see Fig. 7(d) (3 W), irrespective of the output stiffness.

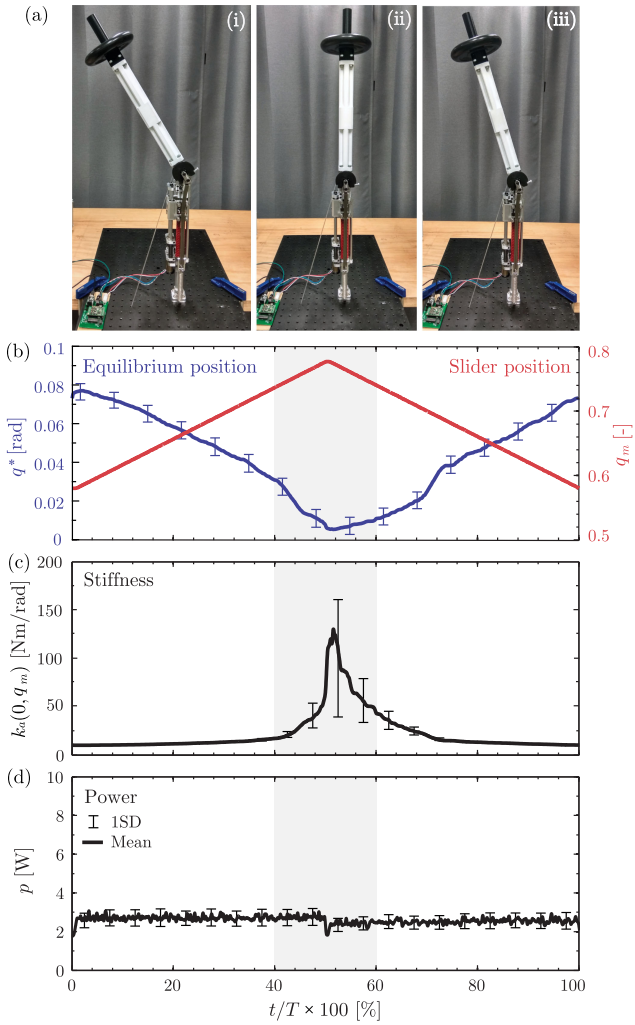

Fig. 7. (a) Stabilization task. (b) Link angle and slider position. (c) Joint stiffness at the trivial equilibrium position $q^* = 0$. (d) Electrical motor power. The plots summarize the data from five repeated experiments. The string, visible in the setup, is carrying an extra weight used to apply a constant moment to the joint.

B. Equilibrium Control Mode

During the swing phase of human locomotion, the knee undergoes initial flexion and subsequent extension. In this section, we aim to demonstrate a similar behavior using equilibrium position control on the knee joint. In the remainder of this section, we consider this to be a swing task.

[5]This formula is valid when the joint angle is small, i.e., $|q| \ll 1$.

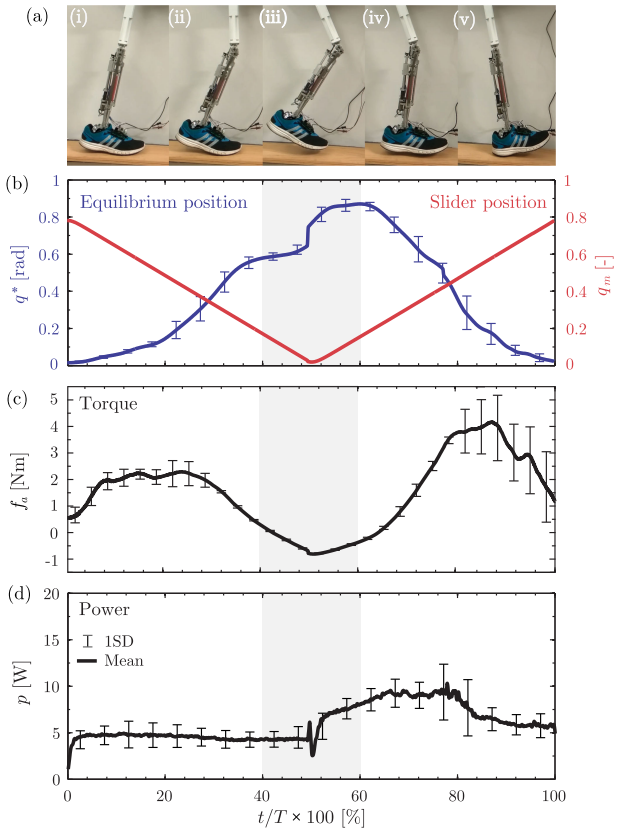

Fig. 8. (a) Swing task. (b) Link angle and slider position. (c) Actuator torque. (d) Electrical motor power. The plots summarize the data from four repeated experiments.

Figure 8 shows the leg, hinged at the hip joint. In order to generate a stepping motion, a torque was provided at the hip using a linear spring pulling the thigh forward, just like the hip torque does in human locomotion. At the initial *push-off* phase, see Fig. 8(a-i), the knee was stiff, i.e., the slider was in high stiffness setting ($q_m = 0.78$). Subsequently, the slider was moved toward lower stiffness settings ($q_m = 0$). As the stiffness reached negative values, a new nontrivial joint equilibrium was generated toward which the limb moved. This resulted in flexion of the knee joint. As the joint flexed, the foot left the ground see Fig. 8(a-ii), and the limb started to move forward, see Fig. 8(a-iii). This was followed by the knee extension motion. In particular, knee extension was achieved by moving the slider toward positive stiffness settings ($q_m \to 1$). This made the trivial equilibrium stable and, correspondingly, caused the knee joint to return to its initial configuration of zero deflection, see Fig. 8(a-iv). The extension phase ended with heel strike see Fig. 8(a-v), and the actuator returned to the stiffness control mode.

This experiment demonstrates the ability of the device to shift the joint equilibrium position to angles up to 60°, see Fig. 8(b) shaded area. This is compatible with normal knee movements during human locomotion [44]. When the device is in equilibrium control mode ($q_m \in [0, 0.6]$), the negative stiffness mechanism provided the force to lift up the leg. This made the knee flex. When the slider was brought back to a high stiffness setting ($q_m \in [0.6, 1]$) the positive stiffness mechanism straightened the knee joint. In the latter case, there was low variation in the equilibrium position see Fig. 8(b), indicating that the actuator was being switched back to the stiffness control mode. We note that our prototype has a limited motion range, although, PNSAs can be designed to have a large motion range. For example, one could use a gear reducer at the output joint to limit the spring deflection to a fraction of the output deflection in the proposed design.

The experimental data shows that the device exhibits two modes of operation. In the stiffness control mode, the joint operated around the origin. As the slider shifted toward high stiffness settings, the output stiffness increased sharply due to the highly nonlinear behavior of the positive stiffness mechanism, and the joint became more rigid. As the slider moved toward low stiffness settings, the device switched to the equilibrium control mode. In this mode, the moment generated by the actuator flexed the joint. We note that precise control of the equilibrium position was nontrivial because of the following reasons: 1) hysteresis between the equilibrium position and the motor position; 2) the limited resolution in the control of the equilibrium position at mode-switching; and 3) the hysteresis in mode switching, which depends on the direction of motion. These limitations are due to the nonlinear force–deflection characteristic of the proposed actuator [35]. These limitations are fundamental; they can be mitigated, but cannot be eliminated by a better design realization of the proposed actuator.

In both of the experiments, we observed low power by the motor, first, during stiffness modulation near to the zero equilibrium position (see Fig. 7(c) and (d) gray 3 W), and second, when the joint was considerably deflected from its equilibrium position (see Fig. 8(a) and (d) gray 15 W). This is because the active positive stiffness mechanism is designed to redirect the forces generated by the leaf-spring to the structure of the actuator instead of the motor unit. In particular, when the leaf spring is not deflected, the force experienced by the driving motor is zero independently of the stiffness. This is partly because the actuator does not need to do considerable amount of work in these tasks, but also because stiffness modulation does not cost considerable amount of energy in this actuator. The latter feature characterizes all previously designed so called energy efficient VSAs [29]. When the leaf spring is deflected, the force experienced by the driving motor is not zero; it is the axial reaction force imposed by the spring on the motor. It can be also shown that the force imposed by the spring on the driving motor remain bounded irrespective of the stiffness. This feature characterizes the class of low-power variable stiffness mechanisms more recently introduced in [20]. This means that the force experienced by the driving motor, and consequently the power drained by the driving motor can be kept low not only when the spring is undeflected but also when it is deflected from its equilibrium configuration.

In summary, the device is able to control stiffness at origin, vary equilibrium position up to a considerable deflection, and switch between these two modes using a single motor. This is achieved without output-feedback, ensuring inherent stable stiffness modulation using the proposed PNSA.

VI. Conclusions

The paper presents a novel compliant actuation concept that combines positive and negative stiffness mechanisms. It is shown that employing a combination of positive and negative stiffness, a compliant actuator is able to modulate its equilibrium position and output stiffness in open-loop fashion using a single motor. Irrespective of how the positive and negative stiffness is generated, as long as the positive stiffness can surpass its negative counterpart, the actuator will exhibit two modes of operation: one allowing control over the equilibrium position, with a predetermined stiffness, and another allowing control over the actuator's stiffness at a fixed stable equilibrium. The former is similar to open-loop equilibrium position modulation in SEAs, while the latter is similar to open-loop stiffness modulation in VSAs.

The proposed actuation concept may find its place in *mechanically adaptable robotic systems* where *stiffness modulation is required but doing large output work by the motor is not required*. For example, it may be used in legged robots, and actuator assisted lower limb prosthetic devices and exoskeletons to provide high knee stiffness in stance, adaptive stiffness at the ankle for efficient walking at different speeds, and negative stiffness at the knee and possibly hip to mimic an ideal ballistic swing [45] without doing considerable work. Further applications include *mechanically adaptive medical braces* that can change stiffness to aid better stability of the biological joint during recovery from injury, and *negative stiffness rehabilitation devices* that can generate joint instability to aid better training and possibly faster recovery after surgery.

Appendix

The parameter that defines the cubic term in (22) is:

$$
\begin{aligned}
k_{\mathrm{I3}}(q_m) = \frac{EI}{L_0}\frac{1}{\delta_m^2}\frac{a}{L_0}\Bigg[& \frac{a}{L_0}(1-q_m)^2\left(2(1-q_m)+9\frac{a}{L_0}\right) \\
& + 6\frac{a}{L_0}\frac{e}{L_0}(1-q_m)\left((1-q_m)+3\frac{a}{L_0}\right) \\
& + 3\frac{a}{L_0}\left(\frac{e}{L_0}\right)^2\left(2(1-q_m)+3\frac{a}{L_0}\right) \\
& + \frac{(F_{e0}-3k_e a)L_0^2}{6EI}(1-q_m)^2\Bigg((1-q_m)^4 \\
& + 6\frac{e}{L_0}(1-q_m)^3 + 15\left(\frac{e}{L_0}\right)^2(1-q_m)^2 \\
& + 18\left(\frac{e}{L_0}\right)^3(1-q_m) + 9\left(\frac{e}{L_0}\right)^4\Bigg)\Bigg]
\end{aligned}
$$

where $\delta_m = [\frac{e}{L_0}+1-q_m]^3 - (\frac{e}{L_0})^3$.

References

[1] A. Bicchi and G. Tonietti, "Fast and soft arm tactics: Dealing with the safety-performance trade-off in robot arms design and control," *IEEE Robot. Automat. Mag.*, vol. 11, no. 2, pp. 22–33, Jun. 2004.

[2] N. Hogan, "Impedance control: An approach to manipulation," *ASME J. Dyn. Syst., Meas. Control*, vol. 107, pp. 1–24, 1985.

[3] G. Pratt and M. Williamson, "Series elastic actuators," in *Proc. IEEE/RSJ Int. Conf. Intell. Robots Syst.*, Pittsburg, PA, USA, 1995, vol. 1, pp. 399–406.

[4] R. van Ham, T. Sugar, B. Vanderborght, K. Hollander, and D. Lefeber, "Compliant actuator designs," *IEEE Robot. Automat. Mag.*, vol. 16, no. 3, pp. 81–94, Sep. 2009.

[5] B. Vanderborght, R. Van Ham, D. Lefeber, T. G. Sugar, and K. W. Hollander, "Comparison of mechanical design and energy consumption of adaptable, passive-compliant actuators," *Int. J. Robot. Res.*, vol. 28, no. 1, pp. 90–103, 2009.

[6] A. M. Dollar and H. Herr, "Lower extremity exoskeletons and active orthoses: Challenges and state-of-the-art," *IEEE Trans. Robot.*, vol. 24, no. 1, pp. 144–158, Feb. 2008.

[7] D. J. Braun *et al.*, "Robots driven by compliant actuators: Optimal control under actuation constraints," *IEEE Trans. Robot.*, vol. 29, no. 5, pp. 1085–1101, Oct. 2013.

[8] J. W. Hurst, J. E. Chestnutt, and A. A. Rizzi, "The actuator with mechanically adjustable series compliance," *IEEE Trans. Robot.*, vol. 26, no. 4, pp. 597–606, Aug. 2010.

[9] N. Hogan, "Adaptive control of mechanical impedance by coactivation of antagonist muscles," *IEEE Trans. Autom. Control*, vol. AC-29, no. 8, pp. 681–690, Aug. 1984.

[10] J. E. Colgate and N. Hogan, "Robust control of dynamically interacting systems," *Int. J. Control*, vol. 48, no. 1, pp. 65–88, 1988.

[11] D. L. Platus, "Negative-stiffness-mechanism vibration isolation systems," *Proc. SPIE*, vol. 1619, pp. 44–54, 1991.

[12] M. T. A. Saif, "On a tunable bistable MEMS theory and experiment," *J. Microelectromechanical Syst.*, vol. 9, no. 2, pp. 157–170, Jun. 2000.

[13] M. Yalcin, B. Uzunoglu, E. Altintepe, and V. Patoglu, "VNSA: Variable negative stiffness actuation based on nonlinear deflection characteristics of buckling beams," in *Proc. IEEE/RSJ Int. Conf. Intell. Robots Syst.*, Tokyo, Japan, Nov. 2013, pp. 5418–5424.

[14] C. B. Churchill, D. W. Shahan, S. P. Smith, A. C. Keefe, and G. P. McKnight, "Dynamically variable negative stiffness structures," *Sci. Advances*, vol. 2, no. 2, 2016, Art. no. e1500778.

[15] S. P. Timoshenko and J. M. Gere, *Theory of Elastic Stability*. New York, NY, USA: MacGraw-Hill, 1961.

[16] D. J. Braun, A. Sutas, and S. Vijayakumar, "Self-tuning bistable parametric feedback oscillator: Near-optimal amplitude maximization without model information," *Physical Rev. E*, vol. 95, 2017, Art. no. 012201.

[17] A. Dahiya and D. J. Braun, "Efficiently tunable positive-negative stiffness actuator," in *Proc. IEEE Int. Conf. Robot. Automat.*, Singapore, May 2017, pp. 1235–1240.

[18] D. J. Braun, S. Apte, O. Adiyatov, A. Dahiya, and N. Hogan, "Compliant actuation for energy efficient impedance modulation," in *Proc. IEEE Int. Conf. Robot. Automat.*, Stockholm, Sweden, May 2016, pp. 636–641.

[19] T.-H. Chong, V. Chalvet, and D. J. Braun, "Analytical conditions for the design of variable stiffness mechanisms," in *Proc. IEEE Int. Conf. Robot. Automat.*, Singapore, May 2017, pp. 1241–1247.

[20] V. Chalvet and D. J. Braun, "Criterion for the design of low power variable stiffness mechanisms," *IEEE Trans. Robot.*, vol. 33, no. 4, pp. 1002–1010, 2017.

[21] H.-F. Lau, A. Sutrisno, T.-H. Chong, and D. J. Braun, "Stiffness Modulator: A Novel Actuator for Human Augmentation," in *Proc. IEEE Int. Conf. Robot. Automat.*, Brisbane, Australia, May 2018, pp. 7742–7748.

[22] M. Cempini, M. Fumagalli, N. Vitiello, and S. Stramigioli, "A clutch mechanism for switching between position and stiffness control of a variable stiffness actuator," in *Proc. IEEE Int. Conf. Robot. Automat.*, Seattle, Washington, USA, May 2015, pp. 1017–1022.

[23] S. Groothuis, R. Carloni, and S. Stramigioli, "Single motor-variable stiffness actuator using bistable switching mechanisms for independent motion and stiffness control," in *Proc. IEEE Int. Conf. Adv. Intell. Mechatronics*, Alberta, Canada, Jul. 2016, pp. 234–239.

[24] T. Morita and S. Sugano, "Design and development of a new robot joint using a mechanical impedance adjuster," in *Proc. IEEE Int. Conf. Robot. Automat.*, Nagoya, Japan, May 1995, vol. 3, pp. 2469–2475.

[25] K. Koganezawa, Y. Watanabe, and N. Shimizu, "Antagonistic muscle-like actuator and its application to multi-dof forearm prosthesis," *Adv. Robot.*, vol. 12, no. 7–8, pp. 771–789, 1997.

[26] C. E. English, "Implementation of variable joint stiffness through antagonistic actuation using rolamite springs," *Mechanism Mach. Theory*, vol. 341, pp. 27–40, 1999.

[27] S. A. Migliore, E. A. Brown, and S. P. DeWeerth, "Novel nonlinear elastic actuators for passively controlling robotic joint compliance," *ASME J. Mech. Des.*, vol. 129, no. 4, pp. 406–412, 2006.

[28] S. Wolf and G. Hirzinger, "A new variable stiffness design: Matching requirements of the next robot generation," in *Proc. IEEE Int. Conf. Robot. Automat.*, Pasadena, CA, USA, May 2008, pp. 1741–1746.
[29] L. C. Visser, R. Carloni, and S. Stramigioli, "Energy-efficient variable stiffness actuators," *IEEE Trans. Robot.*, vol. 27, no. 5, pp. 865–875, Oct. 2011.
[30] J. Choi, S. Hong, W. Lee, S. Kang, and M. Kim, "A robot joint with variable stiffness using leaf springs," *IEEE Trans. Robot.*, vol. 27, no. 2, pp. 229–238, Apr. 2011.
[31] B.-S. Kim and J.-B. Song, "Design and control of a variable stiffness actuator based on adjustable moment arm," *IEEE Trans. Robot.*, vol. 28, no. 5, pp. 1145–1151, Oct. 2012.
[32] A. Jafari, N. G. Tsagarakis, I. Sardellitti, and D. G. Caldwell, "A new actuator with adjustable stiffness based on a variable ratio lever mechanism," *IEEE/ASME Trans. Mechatronics*, vol. 19, no. 1, pp. 55–63, Feb. 2014.
[33] W. Rudin, *Principles of Mathematical Analysis*. New York, NY, USA: McGraw-Hill, 1976.
[34] O. Brune, "Synthesis of a finite two-terminal network whose driving-point impedance is a prescribed function of frequency," *J. Math. Phys.*, vol. 10, no. 1–4, pp. 191–236, 1931.
[35] M. Golubitsky, I. Stewart, and D. Schaeffer, *Singularities and Groups in Bifurcation Theory*. New York, NY, USA: Springer-Verlag, 1988.
[36] S. Timoshenko, *History of Strength of Materials: With a Brief Account of the History of Theory of Elasticity and Theory of Structures*. New York, NY, USA: McGraw-Hill, 1953.
[37] D. Bigoni, F. Dal Corso, F. Bosi, and D. Misseroni, "Eshelby-like forces acting on elastic structures: Theoretical and experimental proof," *Mechanics Mater.*, vol. 80, pp. 368–374, 2015.
[38] R. Van Ham, B. Vanderborght, M. Van Damme, B. Verrelst, and D. Lefeber, "MACCEPA: The mechanically adjustable compliance and controllable equilibrium position actuator: Design and implementation in a biped robot," *Robot. Auton. Syst.*, vol. 55, no. 10, pp. 761–768, 2007.
[39] A. Jafari, N. G. Tsagarakis, and D. G. Caldwell, "A novel intrinsically energy efficient actuator with adjustable stiffness (AwAS)," *IEEE/ASME Trans. Mechatronics*, vol. 18, no. 1, pp. 355–365, Feb. 2013.
[40] S. A. Migliore, E. A. Brown, and S. P. DeWeerth, "Biologically inspired joint stiffness control," in *Proc. IEEE Int. Conf. Robot. Automat.*, Barcelona, Spain, Apr. 2005, pp. 4508–4513.
[41] V. Chalvet and D. J. Braun, "Algorithmic design of low power variable stiffness mechanisms," *IEEE Trans. Robot.*, vol. 33, no. 6, pp. 1508–1515, Dec. 2017.
[42] V. T. Inman, H. J. Ralston, and F. Todd, *Human Walking*. Baltimore, MD, USA: Williams & Wilkins, 1981.
[43] K. Shamaei, G. S. Sawicki, and A. M. Dollar, "Estimation of quasi-stiffness of the human knee in the stance phase of walking," *PLOS One*, vol. 8, no. 3, 2013, Art. no. e59993.
[44] D. Winter, *Biomechanics and Motor Control of Human Movement*. Hoboken, NJ, USA: Wiley, 1990.
[45] S. Mochon and T. A. McMahon, "Ballistic walking: An improved model," *Math. Biosci.*, vol. 52, pp. 241–260, 1980.

David J. Braun (M'09) received the Ph.D. degree in mechanical engineering from Vanderbilt University, Nashville, TN, USA, in 2009.

He is currently an Assistant Professor with the Singapore University of Technology and Design (SUTD), Singapore, where he leads the Dynamics and Control Laboratory. Prior to joining SUTD, he was a Researcher with the Center for Intelligent Mechatronics, Vanderbilt University; the Institute for Robotics and Mechatronics, the German Aerospace Center; and the Statistical Machine Learning and Motor Control Group, the University of Edinburgh. His research interests include compliant actuation, optimal control, and robotics.

Dr. Braun was the recipient of the 2013 IEEE Transactions on Robotics Best Paper Award, he was Scientific Program Co-Chair of the 2015 IEEE International Conference of Robotics and Rehabilitation, and Area Chair of the 2018 Robotics: Science and Systems Conference.

Vincent Chalvet received the Engineering degree in mechatronics from ENSMM, Besancon, France, in 2008, and the Ph.D. degree in automatic control from the Franche-Comte University, Besancon, France, in 2013, where his work was focused on the design, fabrication, and control of robotic micro-electro-mechanical-systems.

He was a Postdoctoral Research Fellow, for two years, with the Dynamics and Control Lab, Singapore University of Technology and Design, where he worked on the design of compliant and energy-efficient robotic systems. He is currently a Postdoc Research Fellow with ENISE, Saint-Etienne, France, working on automatic defect detection of industrial products using vision and artificial intelligence-based technologies.

Abhinav Dahiya received the B.Tech. degree in electrical engineering from the Indian Institute of Technology Roorkee, Roorkee, India, in 2016. From 2016 to 2017, he was a Research Assistant with the Dynamics and Control Laboratory at Singapore University of Technology and Design.

Since 2018, he has been working toward the Ph.D. degree at the University of Waterloo, Waterloo, ON, Canada. His primary focus of study is on task planning for efficient human-robot collaboration. His research interests include robot design, control systems, and higher level task planning.